Received: 16 February 2021 | Revised: 14 April 2021 | Accepted: 28 April 2021

DOI: 10.1111/jfbc.13803

ORIGINAL ARTICLE

Journal of Food Biochemistry WILEY

Enzymatic oxidation of oleuropein and 3-hydroxytyrosol by laccase, peroxidase, and tyrosinase

Jesus Manzano-Nicolas[1] | Amaury Taboada-Rodriguez[1] | Jose Antonio Teruel-Puche[2] | Fulgencio Marin-Iniesta[1] | Francisco Garcia-Molina[3] | Francisco Garcia-Canovas[3] | Jose Tudela-Serrano[3] | Jose Munoz-Munoz[4]

[1]Group of research Food Biotechnology-BTA, Department of Food Technology, Nutrition and Bromatology, Regional Campus of International Excellence "Campus Mare Nostrum", University of Murcia, Murcia, Spain

[2]Group of Molecular Interactions in Membranes, Department of Biochemistry and Molecular Biology-A, Regional Campus of International Excellence "Campus Mare Nostrum", University of Murcia, Murcia, Spain

[3]GENZ-Group of research on Enzymology, Department of Biochemistry and Molecular Biology-A, Regional Campus of International Excellence "Campus Mare Nostrum", University of Murcia, Murcia, Spain

[4]Microbial Enzymology Group (MEG), Department of Applied Sciences, Northumbria University, Newcastle Upon Tyne, UK

Correspondence
Jose Munoz-Munoz, Microbial Enzymology Lab (MEG), Department of Applied Sciences, Northumbria University, Newcastle UponTyne NE1 8ST, Tyne & Wear, UK.
Email: jose.munoz@northumbria.ac.uk

Funding information
Ministerio de Ciencia, Innovacion y Universidades (Madrid, Spain), Grant/Award Number: FEDER RTC-2017-5964-2; Fundacion Seneca (CARM, Murcia, Spain), Grant/Award Number: 20961/PI/18; Murcia University (Murcia, Spain), Grant/Award Number: AEIP-15452; Northumbria University

Abstract

The oxidation of oleuropein and 3-hydroxytyrosol by oxidases laccase, tyrosinase, and peroxidase has been studied. The use of a spectrophotometric method and another spectrophotometric chronometric method has made it possible to determine the kinetic parameters V_{max} and K_M for each enzyme. The highest binding affinity was shown by laccase. The antioxidant capacities of these two molecules have been characterized, finding a very similar primary antioxidant capacity between them. Docking studies revealed the optimal binding position, which was the same for the two molecules and was a catalytically active position.

Practical applications

One of the biggest environmental problems in the food industry comes from olive oil mill wastewater with a quantity of approximately 30 million tons per year worldwide. In addition, olive pomace, the solid residue obtained from the olive oil production, is rich in hydroxytyrosol and oleuropein and the action of enzymatic oxidases can give rise to products in their reactions that can lead to polymerization. This polymerization can have beneficial effects because it can increase the antioxidant capacity with potential application on new functional foods or as feed ingredients. Tyrosinase, peroxidase, and laccase are the enzymes degrading these important polyphenols. The application of a spectrophotometric method for laccase and a chronometric method, for tyrosinase and peroxidase, allowed us to obtain the kinetic information of their reactions on hydroxytyrosol and oleuropein. The kinetic information obtained could advance in the understanding of the mechanism of these important industrial enzymes.

KEYWORDS

3-hydroxytyrosol, laccase, oleuropein, peroxidase, tyrosinase

1 | INTRODUCTION

Oxidases such as laccase (EC 1.10.3.2), tyrosinase (EC 1.14.18.1), and peroxidase (1.11.1.7) act oxidizing reducing agents with oxygen the first two enzymes and hydrogen peroxide by the latest (Tikhonov et al., 2019). Laccase and tyrosinase are two enzymes with copper in their active site, copper proteins (Arregui et al., 2019; Panzella & Napolitano, 2019), while peroxidase has a heme group in its active site (Vlasova, 2018). The products of the three enzymes are unstable, in the case of laccase and peroxidase the products

are free radicals, (Arregui et al., 2019; Vlasova, 2018) which, being very unstable, polymerize. In the same way, the tyrosinase products o-quinones are also very reactive and also polymerize (Panzella & Napolitano, 2019).

The ability of these enzymes to attack phenols, diphenols, and so forth can be used for industrial applications such as wastewater treatment (Bucur et al., 2018; Durán et al., 2002; Janusz et al., 2020; Li et al., 2020). Its action also causes the polymerization of different compounds in a typical fruit of Mediterranean countries such as the olive. This fruit (Xie et al., 2021) has a bitter taste due to a substance called oleuropein (OL) (Ramírez et al., 2014); this compound has in its chemical structure 3-hydroxytyrosol (HT); in the olive processing, OL is transformed into a product that does not have a bitter taste (Ramírez et al., 2014).

On the other hand, one of the biggest environmental problems in the food industry comes from olive oil millwastewater (OMW) with a quantity of approximately 30 million tons per year worldwide (Xie et al., 2021). In addition, olive pomace, the solid residue obtained from the olive oil production (Xie et al., 2020), is rich in HT (Xie et al., 2021) and OL and the action of these oxidases can give rise to products in their reactions that can lead to polymerization, and this polymerization can have beneficial effects because it can increase the antioxidant capacity and therefore increase the health benefits with potential application on new functional foods or as feed ingredients (Xie et al., 2020).

In previous works, we have kinetically characterized the action of laccase, peroxidase, and tyrosinase on a series of substrates (Manzano-Nicolas, Marin-Iniesta, et al., 2020; Manzano-Nicolas, Taboada-Rodriguez, et al., 2020; Rodríguez-López, Fenoll, et al., 2000; Rodríguez-López, Gilabert, et al., 2000). Due to the instability of the products, the activity measurement method used consists of avoiding following these molecules, and this is achieved by using a small amount of ascorbic acid (AH_2) (μM), achieving the reversion of free radicals or *o*-quinones to their original substrate and ascorbic acid is oxidized to dehydroascorbic (Manzano-Nicolas, Marin-Iniesta, et al., 2020; Manzano-Nicolas, Taboada-Rodriguez, et al., 2020; Rodríguez-López, Fenoll, et al., 2000; Rodríguez-López, Gilabert, et al., 2000).

When free radicals or *o*-quinones evolve towards polymerization (more than ten units), new advantages are obtained in these polymers (Xie et al., 2020). Furthermore, this polymerization is done under mild conditions. The polymerization process has been kinetically characterized, and changes and transformations in the structures of the enzymes involved have also been determined (Xie et al., 2021).

Among the compounds present in the olive oil extraction residues, HT and OL are abundant, they have a high capacity as antioxidants, but in the polymer this power becomes greater (Hachicha Hbaieb et al., 2015; Tikhonov et al., 2019). Yield can also be improved by treating oil mill wastewater with fungi such as *Aspergillus niger*, thus achieving a greater release of HT (Hamza et al., 2012), although the fruit ripening process is produced through the action of enzymes such as β-glucosidase, polyphenol oxidase, and peroxidase, increasing the release of OL and a series of enzymes that cause its transformation.

The kinetic characterization of the action of tyrosinase on HT has been carried out with the mushroom enzyme, using MBTH as a coupled reagent, obtaining a value of $K_M = 0.9 \pm 0.07$ mM (Espin-De Gea et al., 2002). The K_M of grape tyrosinase has also been determined with a value of $K_M = 21.6$ mM (García-García et al., 2013).

In this work, the action of these three enzymes: laccase, peroxidase, and tyrosinase on OL and HT substrates will be kinetically studied. This study will allow the kinetic characterization and thus obtain information regarding their mechanisms of action. In addition, the docking studies of these molecules in relation to the different enzymes will allow us to understand these catalytic processes.

2 | MATERIAL AND METHODS

2.1 | Materials

The enzymes employed in this work were Laccase from *Trametes versicolor* (TvL, Fluka 53739, Madrid, Spain, 8 U/mg), Peroxidase from horseradish (Sigma-Aldrich, USA, 251 U/mg), and Tyrosinase or polyphenol oxidase (PPO) from *Agaricus bisporus* (Sigma-Aldrich, USA, 3,130 U/mg). Ascorbic acid (AH_2), 4-tert-butylcatechol (TBC), 3-hydroxytyrosol (HT), and 2,2′-azino-bis(3-ethylbenzothiazoline -6-sulfonic acid) (ABTS) were obtained from Sigma-Aldrich (USA), oleuropein (OL) from Cayman Chemical (USA) (Figure 1), and sodium periodate ($NaIO_4$) from Scharlau (Spain). Stock solutions of the substrates were prepared in 0.15-mM acetic acid or phosphoric acid to prevent auto-oxidation. The buffers used were sodium acetate

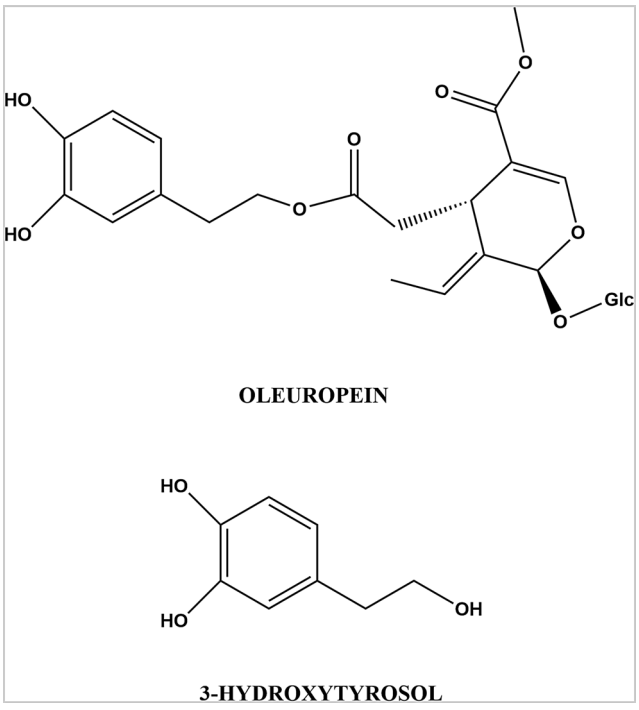

FIGURE 1 Chemical structures of substrates used in this study

(pH 4.0 and 5.5, 50 mM) and sodium phosphate (pH 6.8, 50 mM). Milli-Q system ultrapure water was used.

2.2 | Periodate oxidation of oleuropein and 3-hydroxytyrosol

Periodate oxidation was performed to show the stability and λ_{max} of quinones derivated from OL and HT and calculate its molar absorptivities in the different pH conditions under study. In this sense, the oxidation of target substrates by deficiency of sodium periodate ($NaIO_4$) ($NaIO_4$ <<< Substrate) (Muñoz et al., 2006) was scan recorded at 250–550 nm at 10 min, allowing to (a) select the measurement wavelength in enzymatic assays (λ_{max} or λ_i); (b) calculate molar absorptivity, taking into account the amount of $[NaIO_4]_0$ and the stoichiometric relation of reaction studied; and (c) test the stability of the *o*-quinones produced with the presence or not of decay of absorbance over the time.

2.3 | Enzymatic activity

2.3.1 | Spectrophotometric method

The products of the reaction of these three enzymes (laccase, peroxidase, and tyrosinase) when acting on OL and HT are semiquinones that evolve towards *o*-quinones, in the case of the first two (Manzano-Nicolas, Marin-Iniesta, et al., 2020; Manzano-Nicolas, Taboada-Rodriguez, et al., 2020; Rodríguez-López, Gilabert, et al., 2000) and directly *o*-quinones in the case of tyrosinase (Espín et al., 2001; Muñoz et al., 2006; Rodríguez-López, Fenoll, et al., 2000). It is known that *o*-quinones are unstable, especially at high pH values. Thus, *o*-quinones absorb in the visible region of the spectrum and make it possible to measure the activity of these enzymes; however, their instability means that only laccase can be measured at pH = 4.0, at its optimal pH (Manzano-Nicolas, Marin-Iniesta, et al., 2020; Manzano-Nicolas, Taboada-Rodriguez, et al., 2020). The other two enzymes peroxidase (Rodríguez-López, Gilabert, et al., 2000) and tyrosinase (Rodríguez-López, Fenoll, et al., 2000), which have an optimal pH of 5.5 and 6.8, respectively, cannot be correctly measured, as shown below, in which case a spectrophotometric chronometric method is proposed, as it is described below.

2.3.2 | Chronometric spectrophotometric method

The enzymatic activity of peroxidase and tyrosinase on OL and HT was followed spectrophotometrically in the visible zone, measuring the formation of the corresponding products after the consumption of a determined amount of AH_2 (micromolar) by the reaction with the different quinones and semiquinones generated by the enzymes. Since in all cases the product absorbs in the visible area, the classic chronometric method is used (Muñoz et al., 2006), since the AH_2 spectrum does not influence the measurement (Manzano-Nicolas, Marin-Iniesta, et al., 2020; Manzano-Nicolas, Taboada-Rodriguez, et al., 2020; Rodríguez-López, Fenoll, et al., 2000; Rodríguez-López, Gilabert, et al., 2000). Except where otherwise indicated, the experimental conditions were as follows: pH 5.5 and 50-mM acetate buffer for peroxidase, while pH 6.8 and 50-mM phosphate buffer for tyrosinase; temperature was maintained at 25°C. Substrate and ascorbic acid concentrations are showed in Section 3.

2.3.3 | Antioxidant capacity assays

Antioxidant capacity was obtained through the performing of enzymatic kinetic method (Munoz-Munoz et al., 2010). Experimental conditions of cuvette prepared for measuring antioxidant activity were 50-mM acetate buffer, pH = 5.5, ABTS 5 mM, H_2O_2 100 μM, 0.66-nM peroxidase and 0- to 51-μM OL, and 0- to 56-μM HT. This method consists in the enzymatic production of ABTS radical with its subsequent increase of absorbance. In this way, the addition of different quantities of antioxidant ($[A]_0$) under study produces different lag periods without increase in their absorbance due to the ABTS radical consumption (similarly to previous chronometric method to analyse enzymatic activity). After that, the number of electrons (n) was obtained by calculating for linear regression of $V_0\tau$ respect to $[A]_0$. Finally, effective concentration (EC50 = 1/2n) and antioxidant capacity (ARP = 1/EC50) were obtained.

2.4 | Computational docking

The chemical structures information for all ligands are available in the PubChem Substance and Compound database (Kim et al., 2016) through the unique chemical structure identifier CID 82755 for 3-hydroxytyrosol and 5281544 for oleuropein. The molecular structure of the enzymes was obtained from the Protein Databank: laccase from the Fungus *Trametes versicolor* (PDB ID:1GYC) (Piontek et al., 2002), peroxidase from horseradish (*Armoracia rusticana*, PDB ID:1HCH) (Berglund et al., 2002), and the deoxy-form of tyrosinase from *Agaricus bisporus* (PDB ID:2Y9W, Chain A) (Ismaya et al., 2011). Input protein structures were prepared by adding hydrogen atoms and removing nonfunctional water molecules. Rotatable bonds in the ligands and Gasteiger's partial charges were assigned by AutoDockTools4 software (Morris et al., 2009; Sanner, 1999). The met and oxy forms of tyrosinase were built by a slight modification of the binuclear copper-binding site as previously described (Maria-Solano et al., 2016).

AutoDock 4.2.6 (Morris et al., 2009) package was employed for docking. Lamarkian Genetic Algorithm was chosen to search for the best conformers. The maximum number of energy evaluations was set to 2,500,000, the number of independent docking to 200 and the population size to 150. Grid parameter files were built using AutoGrid 4.2.6 (Huey et al., 2007). The grid box was centered

close to T1 copper for laccase, the copper ions for tyrosinase, and the Fe atom of the heme group. Other AutoDock parameters were used with default values. PyMOL 2.3.0 (Schrödinger, n.d.) and AutoDockTools4 (Morris et al., 2009) were employed to edit and inspect the docked conformations. LigPLot software was used for two-dimensional representations (Wallace et al., 1995). Docking conformations were selected according to the minimum free energy criteria after a cluster analysis in the binding region.

2.5 | Kinetic analysis

To quantitatively measure the rate of action of peroxidase and tyrosinase, it is necessary to obtain an analytical expression for the rate as a function of the parameters obtained experimentally. Similarly, it is necessary, to obtain the antioxidant capacity of a compound by the enzymatic method, to describe an analytical expression that defines it.

2.6 | Spectrophotometric chronometric method for determining the steady-state rate of enzymes

2.6.1 | Peroxidase

Peroxidase (HRP) action on ABTS in presence of AH_2 can be schematized by Figure 2 (Rodríguez-López, Gilabert, et al., 2000).

Therefore, the stoichiometry is as follows: 1 mole of H_2O_2/2 moles of $ABTS^+$/1 mole of AH_2.

In concentration, the quantity of radical formed over time is as follows:

$$V_0 t = [ABTS^{+\cdot}] \quad (1)$$

In presence of AH_2, it happens that:

$$V_0 t - 2[AH_2]_0 = [ABTS^{+\cdot}] \quad (2)$$

In the time, $t = \tau$, results:

$$V_0 \tau = 2[AH_2]_0 \quad (3)$$

$$2ABTS + 1\,H_2O_2 \xrightarrow{POD} 2ABTS^{+\cdot}\,2\,H_2O$$

$$2ABTS^{+\cdot} + 2\,AH_2 \rightarrow 2ABTS + 2AH^{+\cdot}$$

$$2AH^{+\cdot} \rightarrow AH_2 + A$$

FIGURE 2 Action of peroxidase (HRP) on ABTS in presence of AH_2 (Rodríguez-López, Gilabert, et al., 2000)

Therefore

$$V_0 = \frac{2[AH_2]_0}{\tau} = V_{Lag} \quad (4)$$

For a given concentration of AH_2, a lag period is obtained τ, which allows the calculation of V_0, which will be designated as V_{Lag}.

2.6.2 | Tyrosinase

Tyrosinase action on an *o*-diphenol (D) follow the stoichiometry described in Figure 3 (Rodríguez-López, Fenoll, et al., 2000) where the enzyme is saturated by oxygen(Rodríguez-López et al., 1993). In the presence of AH_2, can be schematized by Figure 3.

Therefore, the stoichiometry is 1 mole of O_2/2 moles of D/2 moles of AH_2.

The quantity of quinone accumulated over time is:

$$V_0 t = [Q] \quad (5)$$

In presence of AH_2, the following correlation is achieved:

$$V_0 t - [AH_2]_0 = [Q] \quad (6)$$

In the time, $t = \tau$ results:

$$V_0 \tau = [AH_2]_0 \quad (7)$$

Therefore,

$$V_0 = \frac{[AH_2]_0}{\tau} = V_{Lag} \quad (8)$$

2.7 | Antioxidant capacity determination

Olive oil is rich in antioxidants, such as HT, OL, and oleacin (Czerwińska et al., 2012). It has been shown that tyrosol (T), "the largest constituent in olive oil", restores antioxidant defences despite its weak efficiency as antioxidant (Di Benedetto et al., 2007), probably because of its intracellular accumulation. It has been studied the addition of extra-virgin olive oil on animals diets, reducing the lipid peroxidation by increasing antioxidant defence system

$$2\,D + O_2 \xrightarrow{\text{Tyrosinase (PPO)}} 2\,Q + 2\,H_2O$$

$$2\,Q + 2\,AH_2 \rightarrow 2\,D + 2\,A$$

FIGURE 3 Action of tyrosinase (PPO) on *o*-diphenols in presence of AH_2 (Rodríguez-López, Fenoll, et al., 2000)

(Tufarelli et al., 2016). In general, extra-virgin olive oil enriched diet increase the antioxidant status (Oliveras-López et al., 2013, 2014).

In olive browning reactions, the enzymes tyrosinase and peroxidase intervene, acting mainly on HT (Segovia-Bravo et al., 2009). Given the importance of HT, different methods of obtaining it have been published and even patented (Bernini et al., 2012; Britton et al., 2019; Espin-De Gea et al., 2002).

For the determination of the antioxidant power of OL and HT, the enzymatic kinetic method was used (Munoz-Munoz et al., 2010). The method uses the peroxidase system (POD/ABTS/H_2O_2) to generate the free radical $ABTS^{\cdot+}$, in the presence of an antioxidant, A, the following material balance is met:

$$V_0 t - n[A]_0 = [ABTS^{\cdot+}] \quad (9)$$

where V_0 is the initial rate of action of the enzyme, t, time and n is the number of radical molecules that an antioxidant molecule captures, also called stoichiometric factor. A representation of $V_0\tau$ versus $[A]_0$, according to Equation 9, where τ is the delay period at a given antioxidant concentration, allows to obtain the value of n "stoichiometric factor". From this value, the antioxidant power or capacity (ARP) can be determined.

$$ARP = 2n \quad (10)$$

The effective concentration can also be obtained:

$$EC50 = \frac{1}{2n} \quad (11)$$

This parameter is defined as the ratio of the antioxidant concentration necessary to decrease the initial concentration of radical by 50%.

Therefore, the characterization of the primary antioxidant capacity of a compound is defined by n, EC50 and ARP.

2.8 | Statistical analysis of experimental data

Steady-state rates (V_0 or V_{Lag}) values are determined from the spectrophotometric recordings, and these values are adjusted to the Michaelis–Menten equation through the Sigma Plot program for Windows (Jandel-Scientific, 2016), providing the values of V_{max} and K_M. Data were recorded as mean ± standard deviation of at least triplicate determinations.

3 | RESULTS AND DISCUSSION

The chemical structures of the compounds studied in this work, OL and HT, are shown in Figure 1; note that HT is included in the OL structure.

3.1 | Stability of oleuropein and 3-hydroxytyrosol oxidation products

The oxidation of these compounds by $NaIO_4$ gives the same products as the enzymatic oxidation; therefore, this reagent was used to study the stability at the different optimal pH of the enzymes (laccase pH = 4, peroxidase pH = 5.5 and tyrosinase pH = 6.8) (Muñoz et al., 2006).

3.2 | Oxidation of oleuropein by sodium periodate

In Figure 4 the oxidations of OL by $NaIO_4$ in default are shown at pH = 4 (Figure 4a), pH = 5.5 (Figure 4b), and pH = 6.8 (Figure 4c).

In the spectrophotometric records shown in Figure 4a, a spectrum of OL is shown at pH = 4 (a) and its oxidation product by

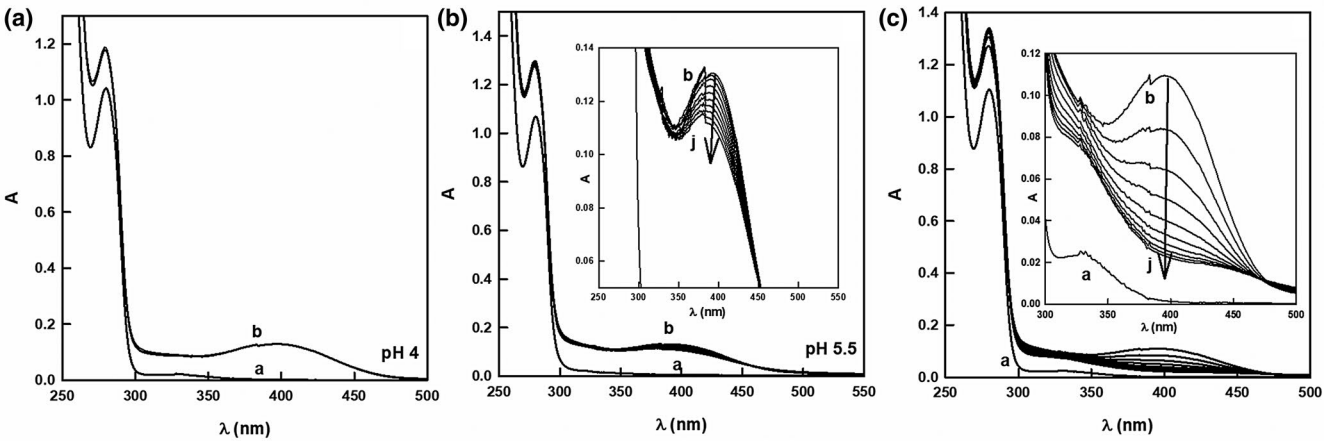

FIGURE 4 Spectrophotometric recordings of oleuropein oxidation by deficiency of $NaIO_4$ at different pH. (a) Oxidation at pH = 4.0. Oleuropein 0.44, 50 mM sodium acetate buffer (recording a) was oxidized with $NaIO_4$, 0.11 mM (recording b). (b) Oxidation at pH = 5.5. Oxidation was done as in (a) but at pH = 5.5. Insert. Variation of absorbance at this pH, the recordings were made every minute (b–j). (c) Oxidation at pH = 6.8. Oxidation was done as in (a) but at pH = 6.8 in 50 mM sodium phosphate buffer. Insert. Variation of absorbance at this pH, the recordings were made every minute (b–j)

deficiency of $NaIO_4$, Figure 4a (Durán et al., 2002). Note the stability of the *o*-quinone at this pH.

In Figure 4b, the oxidation of OL with $NaIO_4$ at pH = 5.5 is shown. In Figure 4b (insert) the instability of *o*-quinone can be seen and this instability becomes greater in Figure 4c and Figure 4c (insert) at pH = 6.8, these processes must be taken into account for the correct determination of the enzymatic activity.

3.3 | Oxidation of 3-hydroxytyrosol by sodium periodate

HT was oxidized by $NaIO_4$ in a 5:1 ratio, with different pH values. Figure S1, HT oxidation at pH = 4.0 is shown giving a stable *o*-quinone. Figure S1b,c shows the spectrophotometric recordings at pH = 5.5 and 6.8 where the instability of the *o*-quinone is demonstrated.

3.4 | Enzymatic oxidation of oleuropein

Figure 5a shows the oxidation of OL with laccase. The product absorbs in the visible zone as in Figure 4a. Figure 5b,c shows the oxidation by peroxidase and tyrosinase, respectively; the instability of *o*-quinone can be appreciated, as occurred in Figure 4b,c.

3.5 | Enzymatic oxidation of 3-hydroxytyrosol at different pH-values

Figure S2 shows the spectrophotometric recordings of the oxidation of HT by laccase, peroxidase and tyrosinase (Figure S2a–c respectively); the spectra are similar to those obtained in Figure S1. It is shown that measurements with laccase can be made at pH = 4.0, measuring the formation of *o*-quinone due to its great stability; however, with peroxidase and tyrosine, as the measurement pH is higher, *o*-quinone is more unstable (Figure S2b,c) and the spectrophotometric chronometric method described in Materials and Methods section should be used.

3.6 | Kinetic characterization of the enzymatic oxidation of oleuropein and 3-hydroxytyrosol

3.6.1 | Kinetic characterization of the enzymatic oxidation of oleuropein

Oxidation of oleuropein by laccase

Figure 6 shows the hyperbolic dependence of the steady-state velocity, V_{SS}, with respect to the OL concentration; the analysis by nonlinear regression to the Michaelis equation allows obtaining $V_{max}^{L,OL}$ and $K_M^{L,OL}$ (L = laccase). Table 1 shows the kinetic parameters of the laccase reaction on HT and OL. Furthermore, they are compared to other *o*-diphenols. From these data, it appears that laccase has the highest affinity for these substrates (see below). The speed of catalysis is related to the values of the chemical shifts of the carbons that support the phenolic hydroxyl group. Furthermore, these data show a greater speed with positively charged substrates in the side chain. Note that when measuring the activity of the enzyme at pH = 4.0, the formation of a fairly stable *o*-quinone is achieved, with which the direct spectrophotometric measurement of *o*-quinone formation is sufficient.

Oxidation of oleuropein by peroxidase

Figure 7 shows the oxidation of OL with peroxidase, in this case, because the optimal pH is 5.5, and according to Figures 4 and 5, *o*-quinone is more unstable than at pH = 4.0; the spectrophotometric chronometric method is used. The experimental recordings necessary to obtain the initial rate are shown in Figure 7

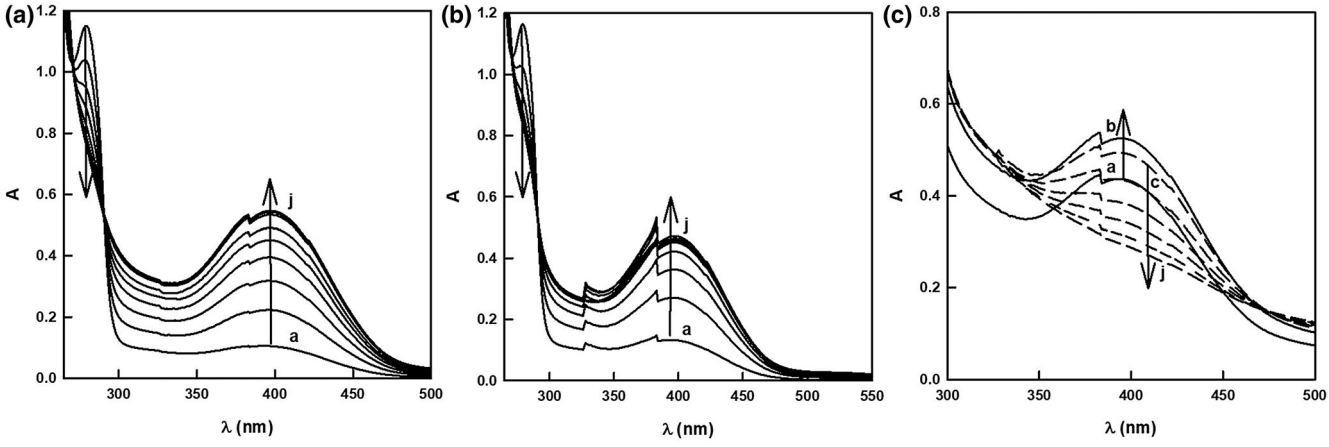

FIGURE 5 Action of laccase, peroxidase and tyrosinase on oleuropein. (a) Action of laccase (17 μg/ml) on oleuropein 0.55 mM in 50-mM sodium acetate buffer, pH = 4; scans were made every minute (a–j). (b) Action of peroxidase (0.65 nM) on oleuropein 0.55 mM at pH = 5.5, scans were made every minute (a–j). (c) Action of tyrosinase (23 nM) on oleuropein 0.55 mM in 50-mM sodium phosphate buffer, pH = 6.8, in recordings a–b, absorbance increases while in recordings c–j, this decreases

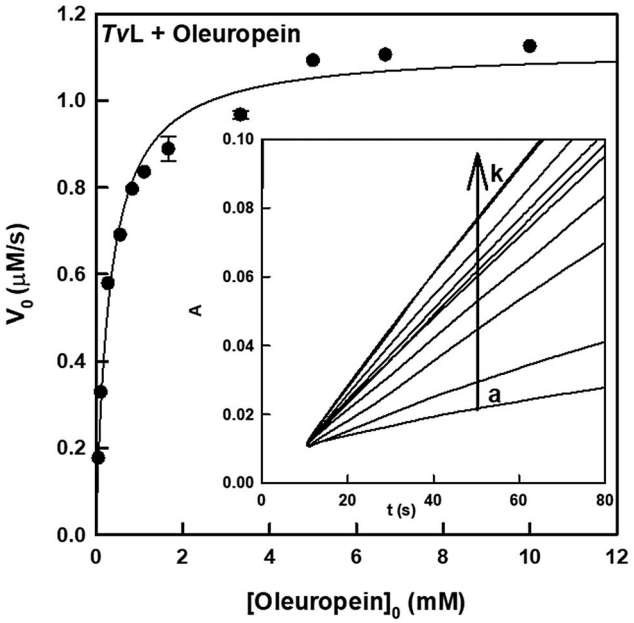

FIGURE 6 Action of laccase on oleuropein. Representation of the steady-state rate values, V_0, obtained by measuring the increase in absorbance over time at $\lambda = 400$ nm. The experimental conditions were as follows: 50-mM sodium acetate buffer, and pH = 4; laccase and oleuropein concentrations were 16.7 μg/ml and (0.056–10 mM), respectively. Insert, Recordings of the increase in absorbance over time. The oleuropein concentrations were (mM): 0.056 (a), 0.11 (b), 0.28 (c), 0.56 (d), 0.83 (e), 1.11 (f), 1.67 (g), 3.33 (h), 5 (i), 6.67 (j), and 10 (k)

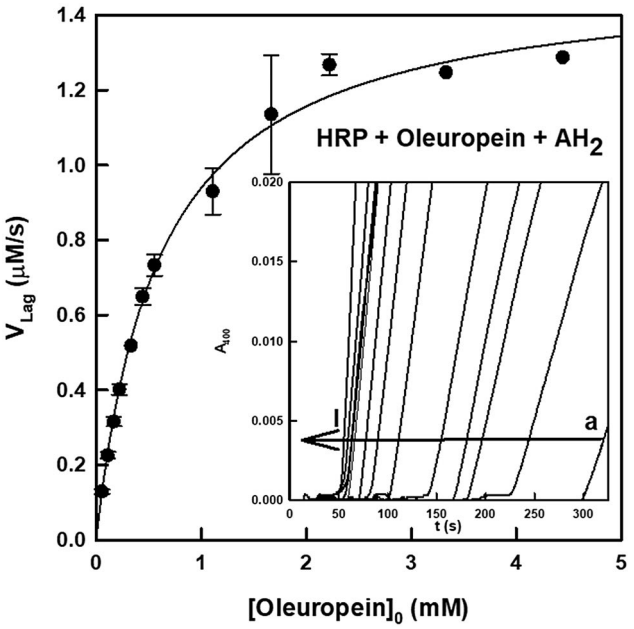

FIGURE 7 Action of peroxidase on oleuropein. Representation of the steady-state rate values obtained with the chronometric method, V_{Lag}, at $\lambda = 400$ nm. Experimental conditions were as follows: 50-mM sodium acetate buffer, pH = 5.5, and $[E]_0 = 0.66$ nM; ascorbic acid 37 μM and oleuropein concentration were varied from 0.056 to 4.44 mM. Insert: spectrophotometric recordings obtained by applying the chronometric method to the action of peroxidase on oleuropein (a–l)

TABLE 1 Parameters and kinetic constants, which characterize the action of laccase on different compounds

Substrate	K_M^S(mM)	V_{max}^S(μM/s)	V_{max}^S/K_M^S (1/h)	δ_3 (ppm)	δ_4 (ppm)	$\delta_{5'}$ (ppm)	$\delta_{6'}$ (ppm)	Reference
L-Epinephrine	0.68 ± 0.04	1.82 ± 0.03	9.66 ± 0.22	143.7	143.7			Manzano-Nicolas, Taboada-Rodriguez, et al. (2020)
L-Norepinephrine	1.09 ± 0.10	1.94 ± 0.07	6.41 ± 0.35	144.0	144.0			Manzano-Nicolas, Marin-Iniesta, et al. (2020)
Dopamine	0.43 ± 0.03	4.86 ± 0.08	41.07 ± 0.29	146.8	145.6			Manzano-Nicolas, Marin-Iniesta, et al. (2020)
3-Hydroxytyrosol	0.18 ± 0.01	0.42 ± 0.01	8.318 ± 0.23	146.15[a]	144.62[a]			This work
Oleuropein	0.31 ± 0.03	1.12 ± 0.03	12.859 ± 0.36			145.2[b]	146.8[b]	This work

[a]Kalampaliki et al. (2019).
[b]Limiroli et al. (1995).

TABLE 2 Parameters and kinetic constants, which characterize the action of peroxidase on different compounds

Substrate	K_M^S(mM)	k_{cat} (s^{-1})	δ_3 (ppm)	δ_4 (ppm)	$\delta_{5'}$ (ppm)	$\delta_{6'}$ (ppm)	Reference
Dopamine	16.8 ± 1.3	447 ± 42	146.86	145.66			Rodríguez-López, Gilabert, et al. (2000)
L-Norepinephrine	8.1 ± 0.70	172 ± 22	146.88	146.88			Rodríguez-López, Gilabert, et al. (2000)
3-Hydroxytyrosol	2.48 ± 0.26	205.52 ± 10.31	146.15[a]	144.62[a]			This work
Oleuropein	0.60 ± 0.04	1,140.91 ± 22.73			145.2[b]	146.8[b]	This work

[a]Kalampaliki et al. (2019).

[b]Limiroli et al. (1995).

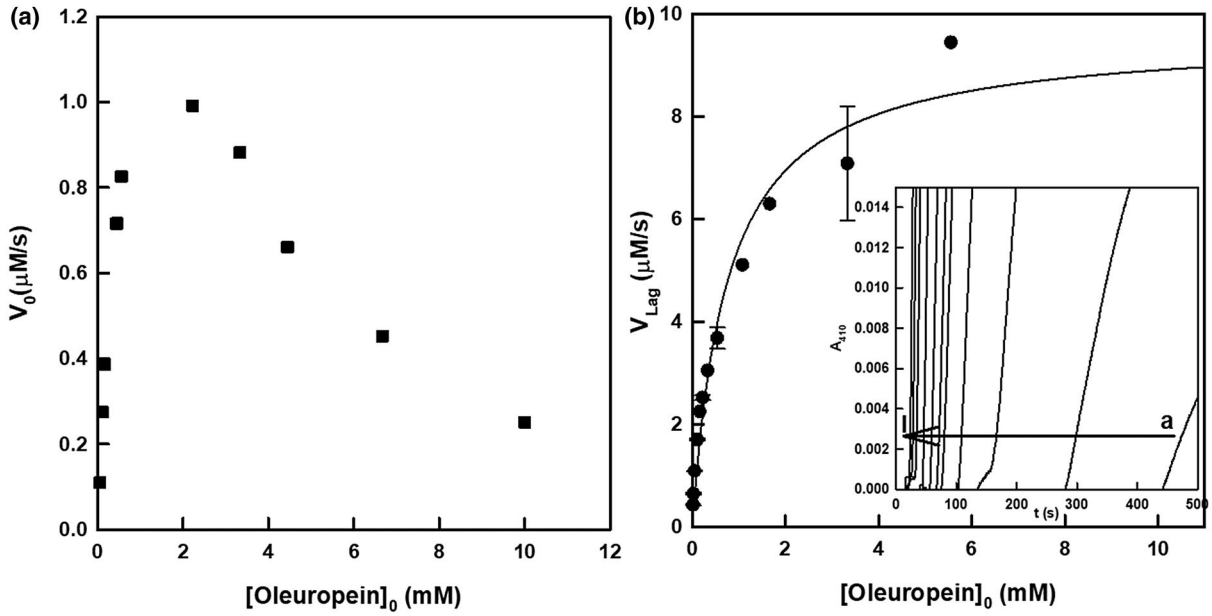

FIGURE 8 Action of tyrosinase on oleuropein. (a) Representation of the apparent steady-state rate values (V_0), obtained measuring the increase in absorbance over time at $\lambda = 400$ nm versus the substrate concentration. (b) Representation of the steady-state rate values obtained with the chronometric method, V_{Lag}, versus oleuropein concentration. Experimental conditions were as follows: 50-mM sodium phosphate buffer, pH = 6.8, and tyrosinase 11 nM, and the oleuropein concentration was varied: (a) 17 μM, (b) 28 μM, (c) 56 μM, (d) 0.111 mM, (e) 0.1667 mM, (f) 0.222 mM, (g) 0.333 mM, (h) 0.5405 mM, (i) 1.08 mM, (j) 1.667 mM, (k) 3.33 mM, and (l) 5.56 mM. (a) In the absence and (b) in presence of ascorbic acid, 85 μM

(insert), starting from the lag period and according to Equation 4 the value of $V_0 = V_{Lag}$ is obtained (for peroxidase acting on oleuropein). From the adjustment of the values of V_{Lag} versus $[OL]_0$, the kinetic parameters $V_{max}^{POD,OL}$ and $K_M^{POD,OL}$ are obtained (Table 2). Note that the values of the chemical displacements are practically the same, and therefore, the k_{cat} values are in the same order; however, the K_M values are lower than the substrates that carry a positive charge in the side chain (dopamine and L-noradrenaline).

Oxidation of oleuropein by tyrosinase

Figure 8a represents the values of V_0, obtained from the increase in absorbance with time, with respect to the concentration of OL, and Figure 8b (insert) shows the spectrophotometric recordings of the absorbance measurement with time, according to the chronometric method. From Equation 8, the values of the initial rate (V_{Lag}) are obtained. From the nonlinear regression adjustment of V_{Lag} versus $[OL]_0$, $V_{max}^{PPO,OL}$ and $K_M^{PPO,OL}$ are obtained, Table 3. The values of the kinetics parameters show that the charged substrates have higher Michaelis constants (K_M^S). The catalytic constants are related to the values of the chemical displacement. In the case of HT, the catalytic constant is higher, because the nucleophilic attack of the C-4 hydroxyl oxygen is more powerful because the value of chemical displacement is lower and therefore the electronic density is higher.

3.7 | Kinetic characterization of 3-hydroxytyrosol oxidation by laccase, peroxidase and tyrosinase

3.7.1 | Oxidation of 3-hydroxytyrosol by laccase, peroxidase and tyrosinase

We followed the same methodology as with OL as shown in Figure S2. For the kinetic characterization of laccase, the spectrophotometric method was used (Figure S3) and with peroxidase

and tyrosinase the spectrophotometric chronometric method was used (Figure S4 Insert and Figure S5 Insert). Figure S4 shows the data obtained with peroxidase according to Equation 4 (V_{Lag}), and Figure S5 shows the values (V_{Lag}) obtained for tyrosinase according to Equation 8. Nonlinear regression analysis to the Michaelis equation of the data in Figures S3–S5 allowed to obtain the kinetic parameters as shown in Tables 1–3.

3.7.2 | Determination of antioxidant capacity of oleuropein and 3-hydroxytyrosol

Figure 9 shows the spectrophotometric recordings of the accumulation of the free radical of ABTS originated in the action of the POD/ABTS/H_2O_2 system in the presence of different concentrations of antioxidant. The parallelism of the records indicates a primary antioxidant power. The data analysis according to Equation 9, allows obtaining the values of V_0 and τ. Figure 9 (insert) shows the relationship of $V_0\tau$ versus $[A]_0$; the slope of this line "*n*" corresponds to the stoichiometric factor between the free radical and the antioxidant. From the value of "*n*", the EC50 parameters (Equation 11) and the antioxidant capacity ARP (Equation 10) can be determined (Table 4). Similar results of the ARP value were obtained with other molecules as has been reported by Muñoz-Muñoz et al., (Munoz-Munoz et al., 2010).

Similar results are obtained with HT (see Table 4). The polymerization of the radicals generated can occur over a long time, increasing the antioxidant capacity (Xie et al., 2020, 2021).

Table 4 shows that the antioxidant capacity of HT and OL are in the same magnitude order than ascorbic acid and Trolox (Munoz-Munoz et al., 2010).

3.8 | Molecular docking study

We have used molecular docking to study binding of HT and OL to laccase, tyrosinase, and peroxidase to identify the interactions of these ligands in the catalytic centre of the enzymes where electron

TABLE 3 Parameters and kinetic constants, which characterize the action of tyrosinase on different compounds

Substrate	K_M^S(mM)	k_{cat} (s^{-1})	δ_3 (ppm)	δ_4 (ppm)	$\delta_{5'}$ (ppm)	$\delta_{6'}$ (ppm)	Reference
Dopamine	2.2 ± 0.1	439.0 ± 17.6	146.86	145.66			Rodríguez-López, Fenoll, et al. (2000)
L-Dopa	0.8 ± 0.03	107.4 ± 3.1	146.92	146.06			Rodríguez-López, Fenoll, et al. (2000)
3-Hydroxytyrosol	0.57 ± 0.04	632.04 ± 13.24	146.15[a]	144.62[a]			This work
Oleuropein	0.76 ± 0.09	422.89 ± 18.01			145.2[b]	146.8[b]	This work

[a]Kalampaliki et al. (2019).
[b]Limiroli et al. (1995).

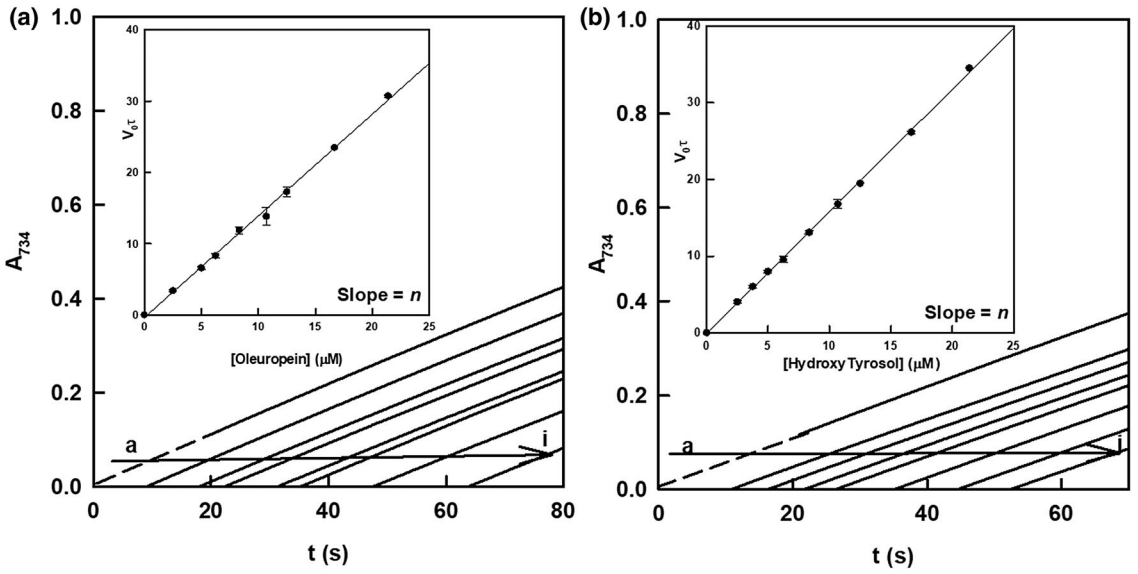

FIGURE 9 Characterization of oleuropein and 3-Hydroxytyrosol antioxidant activity. Time course of $ABTS^{\cdot+}$ accumulation in the presence of peroxidase (0.22 nM), ABTS (5 mM) and H_2O_2 (0.1 mM) in 50-mM sodium acetate buffer, pH = 5.5, at 25°C. The reaction was followed by measuring the increases of absorbance at 734 nm. (a) Oleuropein. Recording (a), control, recordings (b–i) were the same reaction but adding oleuropein 1.25, 2.5, 3.75, 5, 6.25, 8.33, 10.69, 12.5, 16.67, and 21.39 μM, respectively. Insert. Representation of $V_0\tau$ versus $[\text{oleuropein}]_0$. (b) 3-Hydroxytyrosol. Recording (a), control, recordings (b–i) were the same reaction but adding 3-Hydroxytyrosol 1.25, 2.5, 3.75, 5, 6.25, 8.33, 10.69, 12.5, 16.67, and 21.39 μM, respectively. Insert. Representation of $V_0\tau$ versus $[\text{3-Hydroxytyrosol}]_0$

transfer from substrates to the enzymes can take place for catalysis. Equilibrium dissociation constants from docking results are shown in Table 5.

HT and OL bind similarly to the active center of laccase from fungus *Trametes versicolor* through the *o*-diphenol group as seen in Figure 10. The main amino acid residues involved in the interactions with the *o*-diphenol groups are His458 and Asp206 by hydrogen bonds to the phenol groups and Phe265 by Π-interactions with the aromatic rings. Other hydrogen bonds are formed between Pro163 and 3-hydroxytyrosol and between Gly334 and Gly39 and oleuropein. Besides, Phe332 is close enough to present hydrophobic interactions with oleuropein. Thus, the number of interactions of oleuropein

TABLE 4 Characterization of the antioxidant capacity of different compounds

Compound	n (electrons)	EC50	ARP	Reference
L-ascorbic acid	2.01 ± 0.12	0.25 ± 0.03	4.00 ± 0.21	Munoz-Munoz et al. (2010)
Trolox	1.98 ± 0.12	0.25 ± 0.03	4.00 ± 0.24	Munoz-Munoz et al. (2010)
3-Hydroxytyrosol	1.59 ± 0.01	0.31 ± 0.00	3.19 ± 0.02	This work
Oleuropein	1.43 ± 0.02	0.35 ± 0.00	2.86 ± 0.04	This work

TABLE 5 Equilibrium dissociation constants obtained from ligands docking

Compound	Laccase (mM)	Tyrosinase (met-form) (mM)	Tyrosinase (oxy-form) (mM)	Peroxidase (mM)
3-Hydroxytyrosol	0.52	0.54	3.6	0.32
Oleuropein	0.04	0.01	1	0.05

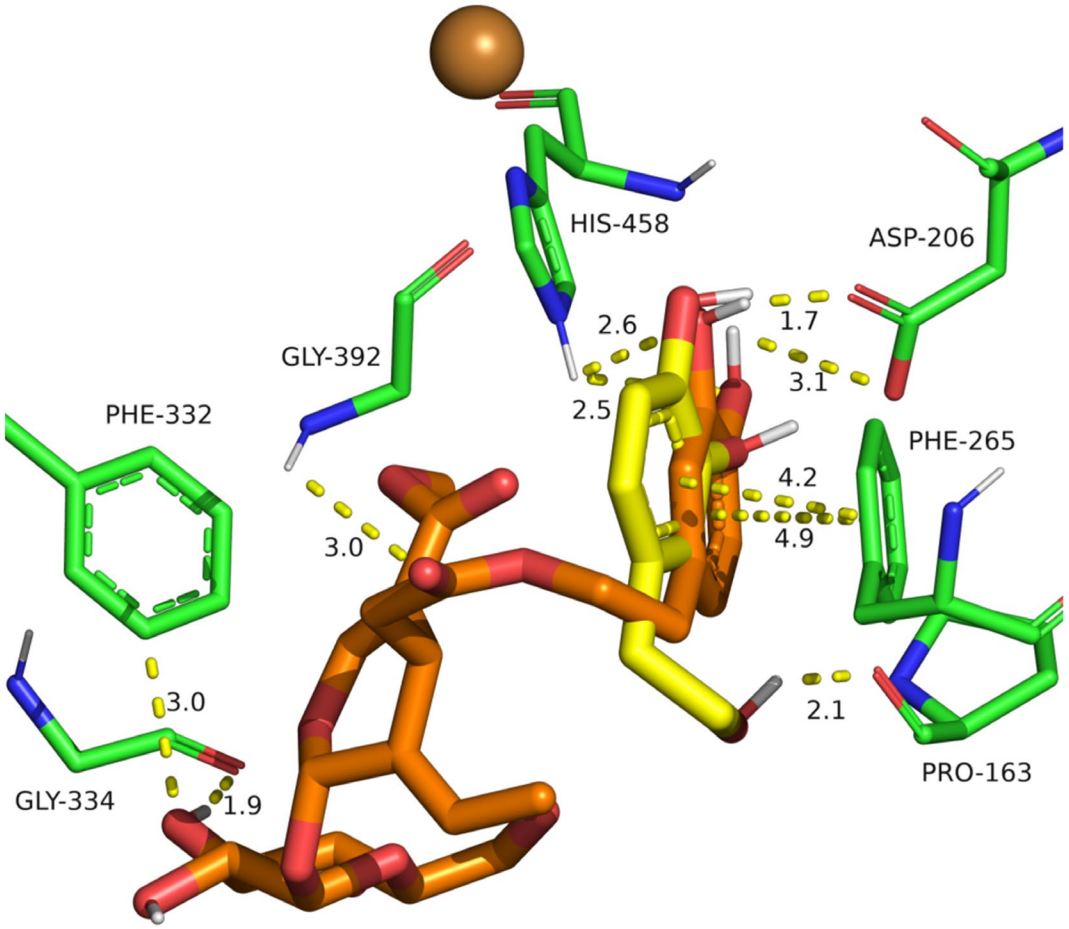

FIGURE 10 Docked conformations of 3-hydroxytyrosol and oleuropein in the laccase 1GYC model. The conformers only include polar hydrogens. The brown sphere corresponds to the metal ion (T1 copper). Carbon backbone is depicted in green in the laccase residues, yellow in 3OHT, and orange in oleuropein. Other atom colors are as follows: red = oxygen, blue = nitrogen, and white = hydrogen. Distances (Å) are shown in yellow dashed lines

with laccase is greater than in the case of 3-hydroxytyrosol yielding a lower K_d for oleuropein (Table 5). A 2D view of these results is shown in Figures S6 and S7. Our docking results with laccase are in good agreement with previously reported works, where participation of His458 and Asp206 in hydrogen bonds formation with substrates of laccase (Madzak et al., 2006; Manzano-Nicolas, Taboada-Rodriguez, et al., 2020; Piontek et al., 2002; Polyakov et al., 2019), and Π-interactions of substrates with Phe265 have been suggested (Manzano-Nicolas, Taboada-Rodriguez, et al., 2020).

Tyrosinase carries out two consecutive reactions in the presence of molecular oxygen: hydroxylation of monophenols to form *o*-diphenols by the oxy-form of tyrosinase and oxidation of *o*-diphenols to *o*-quinones by the met-form of tyrosinase that the oxy-form of tyrosinase can also oxidize *o*-diphenols to *o*-quinones (Zolghadri et al., 2019). Therefore, HT and OL docking have been done to both the met-form and the oxy-form of tyrosinase.

HT and OL binding to the met-form of tyrosinase from *Agaricus bisporus* shows a full overlap of the diphenol group of both ligands (Figure 11). The main interactions of tyrosinase with the diphenol groups are from copper ions, the hydroxyl group, and Phe264 residue by hydrogen bonds, from His263 residue by Π-interactions with the aromatic rings and from Val283 residue by hydrophobic interactions (Figure S8). Besides, OL presents additional hydrogen bonds to Asp191 and Glu189 residues (Figure S9). Again, the number of interactions in OL is greater than in HT yielding a lower K_d for OL (Table 5). A 2D view of these results is shown in Figures S8 and S9. Similar results for binding of other ligands to tyrosinase have been reported from docking studies (Garcia-Jimenez et al., 2016; Nokinsee et al., 2015).

Ligands binding to the oxy-form of tyrosinase are shown in Figure S10 where a good overlap of the diphenols groups is observed. Hydrogen bonds are formed from the molecular oxygen to the diphenol groups. The aromatic ring position of the diphenol groups is stabilized by Π-interactions from His263 and by hydrophobic interactions with Val283. The OL tail is further stabilized by hydrogen bonds interactions with Asn260, Thr261, and Arg268 and by hydrophobic interactions with Val248 (Figure S10). It is to note that in the case of oxy-form, there are no interactions from the ligands to the copper

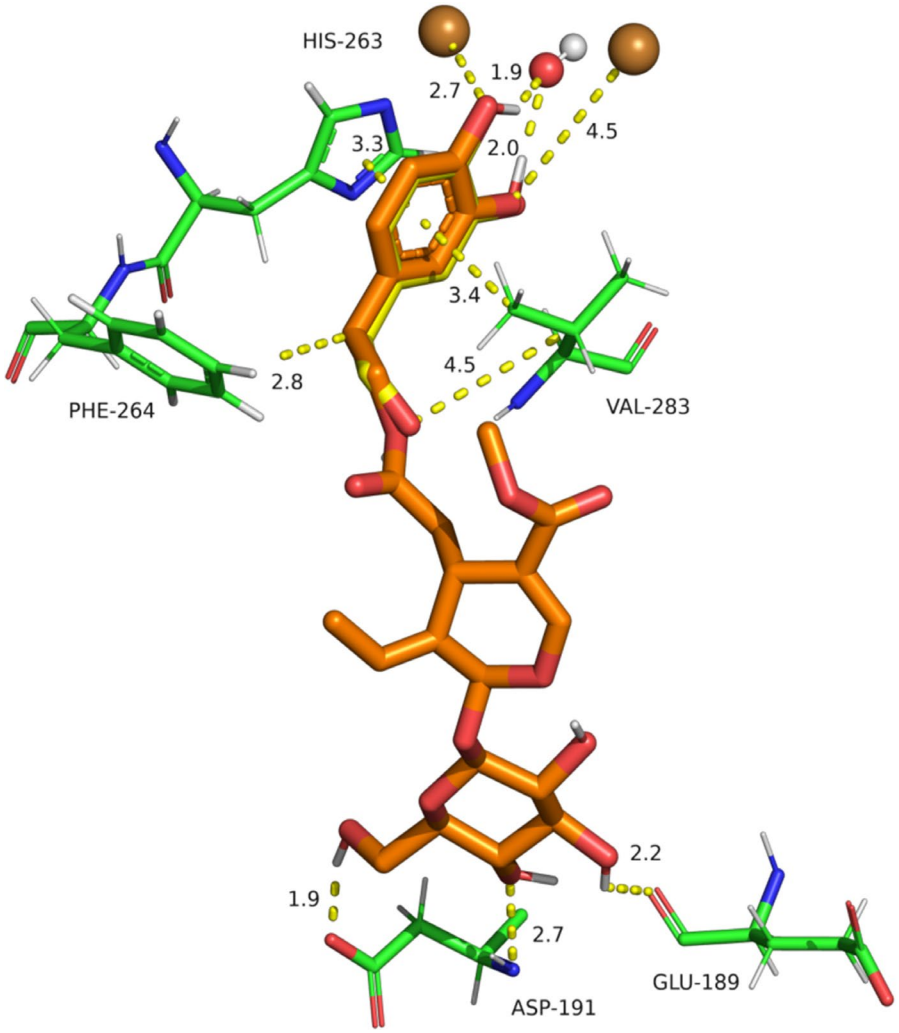

FIGURE 11 Docked conformations of 3-hydroxytyrosol and oleuropein in the met-form of *Agaricus bisporus* tyrosinase. Color scheme as in Figure 10

atoms but to the oxygen atoms of molecular oxygen. The number of interactions in oleuropein is greater than in HT yielding a lower K_d for OL (Table 5). A 2D view of these results is shown in Figures S11 and S12. Similar results have been reported for binding of other ligands to the oxy-form of tyrosinase (Garcia-Jimenez et al., 2018).

HT and OL bind similarly to the active center of horseradish peroxidase through the diphenol groups as seen in Figure S13. The amino acid residues involved in the interactions with the diphenol groups are the iron atom of the heme group and His42 and Ser73 residues by electrostatic interactions including hydrogen bonds. Involvement of His42 and Ser73 residues in ligand binding to the catalytic site of horseradish peroxidase has also been previously reported (Mahfoudi et al., 2017; Sangha et al., 2016). HT also shows hydrogen bond with Arg38 residue. Moreover, OL shows hydrogen bonds with Arg178 and Asp182 and hydrophobic interactions with Gly69 and Leu138 (Figure S13). Thereby, the number of interactions of OL with peroxidase is greater than in the case of HT yielding a lower Kd for OL (Table 5). A 2D view of these results is shown in Figures S14 and S15.

4 | CONCLUSIONS

The action of laccase, peroxidase, and tyrosinase on OL and HT has been kinetically characterized using a spectrophotometric method for laccase and another spectrophotometric chronometric method for peroxidase and tyrosinase. Applying these methods shows that the highest affinity by these compounds corresponds to laccase. The two compounds have a similar antioxidant capacity, which could indicate that the active part of OL corresponds to HT. The docking studies of the three enzymes reveal a similar action of these enzymes on these two molecules.

These results open the possibility of preferentially using laccase in the treatment of oleuropein-rich food industry waste for its decontamination and for obtaining healthy products with potential use as raw materials in pharmacy or as ingredients for functional food and feed.

ACKNOWLEDGMENTS

This work was partially supported by several grants, FEDER RTC-2017-5964-2 InsectFlour project "Aprovechamiento de subproductos industriales agrícolas para la producción de harinas de insectos para consumo humano y animal"/"Exploitation of industrial agronomic by-products to the production of insect flours for human and animal consumption" from Ministerio de Ciencia, Innovacion y Universidades (Madrid, Spain), 20961/PI/18 project from Fundacion Seneca (CARM, Murcia, Spain), and AEIP-15452 project from Murcia University (Murcia, Spain). J. M.-M. has funding from internal grants in Northumbria University.

CONFLICT OF INTEREST

The authors declared that they have no conflict of interest.

AUTHOR CONTRIBUTIONS

Jesus Manzano-Nicolas: Conceptualization; Data curation; Investigation; Methodology; Writing-review & editing. **Amaury Taboada:** Formal analysis; Investigation; Writing-review & editing. **Jose Antonio Teruel-Puche:** Investigation; Methodology; Writing-original draft. **Fulgencio Marin-Iniesta:** Funding acquisition; Methodology; Project administration; Resources; Writing-original draft. **Francisco Garcia-Molina:** Formal analysis; Methodology; Writing-original draft; Writing-review & editing. **Francisco Garcia-Canovas:** Conceptualization; Data curation; Formal analysis; Investigation; Methodology; Supervision; Validation; Writing-original draft; Writing-review & editing. **Jose Tudela:** Data curation; Supervision; Validation; Visualization; Writing-review & editing. **Jose Munoz-Munoz:** Conceptualization; Data curation; Formal analysis; Investigation; Methodology; Project administration; Supervision; Validation; Visualization; Writing-original draft; Writing-review & editing.

ORCID

Jesus Manzano-Nicolas https://orcid.org/0000-0002-7619-218X
Amaury Taboada-Rodriguez https://orcid.org/0000-0003-0832-0108
Jose Antonio Teruel-Puche https://orcid.org/0000-0003-2256-3368
Fulgencio Marin-Iniesta https://orcid.org/0000-0002-9642-0266
Francisco Garcia-Molina https://orcid.org/0000-0003-4481-7568
Francisco Garcia-Canovas https://orcid.org/0000-0002-8869-067X
Jose Tudela-Serrano https://orcid.org/0000-0002-5528-4296
Jose Munoz-Munoz https://orcid.org/0000-0003-0010-948X

REFERENCES

Arregui, L., Ayala, M., Gómez-Gil, X., Gutiérrez-Soto, G., Hernández-Luna, C. E., Herrera de los Santos, M., Levin, L., Rojo-Domínguez, A., Romero-Martínez, D., Saparrat, M. C. N., Trujillo-Roldán, M. A., & Valdez-Cruz, N. A. (2019). Laccases: Structure, function, and potential application in water bioremediation. *Microbial Cell Factories*, *18*(1), 200. https://doi.org/10.1186/s12934-019-1248-0

Berglund, G. I., Carlsson, G. H., Smith, A. T., Szöke, H., Henriksen, A., & Hajdu, J. (2002). The catalytic pathway of horseradish peroxidase at high resolution. *Nature*, *417*(6887), 463–468. https://doi.org/10.1038/417463a

Bernini, R., Crisante, F., Barontini, M., Tofani, D., Balducci, V., & Gambacorta, A. (2012). Synthesis and structure/antioxidant activity relationship of novel catecholic antioxidant structural analogues to hydroxytyrosol and its lipophilic esters. *Journal of Agricultural and Food Chemistry*, *60*(30), 7408–7416. https://doi.org/10.1021/jf301131a

Britton, J., Davis, R., & O'Connor, K. E. (2019). Chemical, physical and biotechnological approaches to the production of the potent antioxidant hydroxytyrosol. *Applied Microbiology and Biotechnology*, *103*(15), 5957–5974. https://doi.org/10.1007/s00253-019-09914-9

Bucur, B., Munteanu, F.-D., Marty, J.-L., & Vasilescu, A. (2018). Advances in enzyme-based biosensors for pesticide detection. *Biosensors*, *8*(2), 27.–https://doi.org/10.3390/bios8020027

Czerwińska, M., Kiss, A. K., & Naruszewicz, M. (2012). A comparison of antioxidant activities of oleuropein and its dialdehydic derivative from olive oil, oleacein. *Food Chemistry*, *131*(3), 940–947. https://doi.org/10.1016/j.foodchem.2011.09.082

Di Benedetto, R., Varì, R., Scazzocchio, B., Filesi, C., Santangelo, C., Giovannini, C., Matarrese, P., D'Archivio, M., & Masella, R. (2007). Tyrosol, the major extra virgin olive oil compound, restored intracellular antioxidant defences in spite of its weak antioxidative effectiveness. *Nutrition, Metabolism and Cardiovascular Diseases*, *17*(7), 535–545. https://doi.org/10.1016/j.numecd.2006.03.005

Durán, N., Rosa, M. A., D'Annibale, A., & Gianfreda, L. (2002). Applications of laccases and tyrosinases (phenoloxidases) immobilized on different supports: A review. *Enzyme and Microbial Technology*, *31*(7), 907–931. https://doi.org/10.1016/S0141-0229(02)00214-4

Espín, J. C., Soler-Rivas, C., Cantos, E., Tomás-Barberán, F. A., & Wichers, H. J. (2001). Synthesis of the antioxidant hydroxytyrosol using tyrosinase as biocatalyst. *Journal of Agricultural and Food Chemistry*, *49*(3), 1187–1193. https://doi.org/10.1021/jf001258b

Espin-De Gea, J. C., De Tomas-Barberan, F. A., Garcia-Viguera, M. C., Ferreres-De Arce, F., Soler-Rivas, C., & Wichers, H. J. (2002). *Enzymatic synthesis of antioxidant hydroxytyrosol* (Patent No. WO 02/16628 A1). https://digital.csic.es/bitstream/10261/31074/1/WO0216628A1.pdf

García-García, M. I., Hernández-García, S., Sánchez-Ferrer, Á., & García-Carmona, F. (2013). Kinetic study of hydroxytyrosol oxidation and its related compounds by red globe grape polyphenol oxidase. *Journal of Agricultural and Food Chemistry*, *61*(25), 6050–6055. https://doi.org/10.1021/jf4009422

Garcia-Jimenez, A., García-Molina, F., Teruel-Puche, J. A., Saura-Sanmartin, A., Garcia-Ruiz, P. A., Ortiz-Lopez, A., Rodríguez-López, J. N., Garcia-Canovas, F., & Munoz-Munoz, J. (2018). Catalysis and inhibition of tyrosinase in the presence of cinnamic acid and some of its derivatives. *International Journal of Biological Macromolecules*, *119*, 548–554. https://doi.org/10.1016/j.ijbiomac.2018.07.173

Garcia-Jimenez, A., Teruel-Puche, J. A., Ortiz-Ruiz, C. V., Berna, J., Tudela, J., & Garcia-Canovas, F. (2016). 4-n-butylresorcinol, a depigmenting agent used in cosmetics, reacts with tyrosinase. *IUBMB Life*, *68*(8), 663–672. https://doi.org/10.1002/iub.1528

Hachicha Hbaieb, R., Kotti, F., García-Rodríguez, R., Gargouri, M., Sanz, C., & Pérez, A. G. (2015). Monitoring endogenous enzymes during olive fruit ripening and storage: Correlation with virgin olive oil phenolic profiles. *Food Chemistry*, *174*, 240–247. https://doi.org/10.1016/j.foodchem.2014.11.033

Hamza, M., Khoufi, S., & Sayadi, S. (2012). Fungal enzymes as a powerful tool to release antioxidants from olive mill wastewater. *Food Chemistry*, *131*(4), 1430–1436. https://doi.org/10.1016/j.foodchem.2011.10.019

Huey, R., Morris, G. M., Olson, A. J., & Goodsell, D. S. (2007). A semiempirical free energy force field with charge-based desolvation. *Journal of Computational Chemistry*, *28*(6), 1145–1152. https://doi.org/10.1002/jcc.20634

Ismaya, W. T., Rozeboom, H. J., Schurink, M., Boeriu, C. G., Wichers, H., & Dijkstra, B. W. (2011). Crystallization and preliminary X-ray crystallographic analysis of tyrosinase from the mushroom *Agaricus bisporus*. *Acta Crystallographica Section F(Crystallization Communications)*, *F67*, 575–578.

Jandel-Scientific. (2016). Sigma Plot for WindowsTM, Corte Madera.

Janusz, G., Pawlik, A., Świderska-Burek, U., Polak, J., Sulej, J., Jarosz-Wilkołazka, A., & Paszczyński, A. (2020). Laccase properties, physiological functions, and evolution. *International Journal of Molecular Sciences*, *21*, 966. https://doi.org/10.3390/ijms21030966

Kalampaliki, A. D., Giannouli, V., Skaltsounis, A.-L., & Kostakis, I. K. (2019). A three-step, gram-scale synthesis of hydroxytyrosol, hydroxytyrosol acetate, and 3,4-dihydroxyphenylglycol. *Molecules*, *24*, 3239. https://doi.org/10.3390/molecules24183239

Kim, S., Thiessen, P. A., Bolton, E. E., Chen, J., Fu, G., Gindulyte, A., Han, L., He, J., He, S., Shoemaker, B. A., Wang, J., Yu, B., Zhang, J., & Bryant, S. H. (2016). PubChem substance and compound databases. *Nucleic Acids Research*, *44*(D1), D1202–D1213. https://doi.org/10.1093/nar/gkv951

Li, X., Li, S., Liang, X., McClements, D. J., Liu, X., & Liu, F. (2020). Applications of oxidases in modification of food molecules and colloidal systems: Laccase, peroxidase and tyrosinase. *Trends in Food Science & Technology*, *103*, 78–93. https://doi.org/10.1016/j.tifs.2020.06.014

Limiroli, R., Consonni, R., Ottolina, G., Marsilio, V., Bianchi, G., & Zetta, L. (1995). 1H and 13C NMR characterization of new oleuropein aglycones. *Journal of the Chemical Society, Perkin Transactions*, *1*(12), 1519–1523. https://doi.org/10.1039/P19950001519

Madzak, C., Mimmi, M. C., Caminade, E., Brault, A., Baumberger, S., Briozzo, P., Mougin, C., & Jolivalt, C. (2006). Shifting the optimal pH of activity for a laccase from the fungus *Trametes versicolor* by structure-based mutagenesis. *Protein Engineering, Design and Selection*, *19*(2), 77–84. https://doi.org/10.1093/protein/gzj004

Mahfoudi, R., Djeridane, A., Benarous, K., Gaydou, E. M., & Yousfi, M. (2017). Structure-activity relationships and molecular docking of thirteen synthesized flavonoids as horseradish peroxidase inhibitors. *Bioorganic Chemistry*, *74*, 201–211. https://doi.org/10.1016/j.bioorg.2017.08.001

Manzano-Nicolas, J., Marin-Iniesta, F., Taboada-Rodriguez, A., Garcia-Canovas, F., Tudela-Serrano, J., & Muñoz-Muñoz, J. L. (2020). Development of a method to measure laccase activity on methoxyphenolic food ingredients and isomers. *International Journal of Biological Macromolecules*, *151*, 1099–1107. https://doi.org/10.1016/j.ijbiomac.2019.10.152

Manzano-Nicolas, J., Taboada-Rodriguez, A., Teruel-Puche, J.-A., Marin-Iniesta, F., Garcia-Molina, F., Garcia-Canovas, F., Tudela-Serrano, J., & Muñoz-Muñoz, J.-L. (2020). Kinetic characterization of the oxidation of catecolamines and related compounds by laccase. *International Journal of Biological Macromolecules*, *164*, 1256–1266. https://doi.org/10.1016/j.ijbiomac.2020.07.112

Maria-Solano, M. A., Ortiz-Ruiz, C. V., Muñoz-Muñoz, J. L., Teruel-Puche, J. A., Berna, J., Garcia-Ruiz, P. A., & Garcia-Canovas, F. (2016). Further insight into the pH effect on the catalysis of mushroom tyrosinase. *Journal of Molecular Catalysis B: Enzymatic*, *125*, 6–15. https://doi.org/10.1016/j.molcatb.2015.12.008

Morris, G. M., Huey, R., Lindstrom, W., Sanner, M. F., Belew, R. K., Goodsell, D. S., & Olson, A. J. (2009). AutoDock4 and AutoDockTools4: Automated docking with selective receptor flexibility. *Journal of Computational Chemistry*, *30*(16), 2785–2791. https://doi.org/10.1002/jcc.21256

Muñoz, J. L., García-Molina, F., Varón, R., Rodriguez-Lopez, J. N., García-Cánovas, F., & Tudela, J. (2006). Calculating molar absorptivities for quinones: Application to the measurement of tyrosinase activity. *Analytical Biochemistry*, *351*(1), 128–138. https://doi.org/10.1016/j.ab.2006.01.011

Munoz-Munoz, J. L., Garcia-Molina, F., Varon, R., Tudela, J., García-Cánovas, F., & Rodriguez-Lopez, J. N. (2010). Quantification of the antioxidant capacity of different molecules and their kinetic antioxidant efficiencies. *Journal of Agricultural and Food Chemistry*, *58*(4), 2062–2070. https://doi.org/10.1021/jf9042024

Nokinsee, D., Shank, L., Lee, V. S., & Nimmanpipug, P. (2015). Estimation of inhibitory effect against tyrosinase activity through homology modeling and molecular docking. *Enzyme Research*, *2015*, 1–12. https://doi.org/10.1155/2015/262364

Oliveras-López, M.-J., Berná, G., Jurado-Ruiz, E., López-García de la Serrana, H., & Martín, F. (2014). Consumption of extra-virgin olive oil rich in phenolic compounds has beneficial antioxidant effects in healthy human adults. *Journal of Functional Foods*, *10*, 475–484. https://doi.org/10.1016/j.jff.2014.07.013

Oliveras-López, M.-J., Molina, J. J. M., Mir, M. V., Rey, E. F., Martín, F., & de la Serrana, H.- L.-G. (2013). Extra virgin olive oil (EVO) consumption and antioxidant status in healthy institutionalized elderly humans. *Archives of Gerontology and Geriatrics*, *57*(2), 234–242. https://doi.org/10.1016/j.archger.2013.04.002

Panzella, L., & Napolitano, A. (2019). Natural and bioinspired phenolic compounds as tyrosinase inhibitors for the treatment of skin hyperpigmentation: Recent advances. *Cosmetics*, *6*(4), 57. https://doi.org/10.3390/cosmetics6040057

Piontek, K., Antorini, M., & Choinowski, T. (2002). Crystal structure of a laccase from the fungus *Trametes versicolor* at 1.90-Å resolution containing a full complement of coppers. *Journal of Biological Chemistry*, *277*(40), 37663–37669. https://doi.org/10.1074/jbc.M204571200

Polyakov, K. M., Gavryushov, S., Fedorova, T. V., Glazunova, O. A., & Popov, A. N. (2019). The subatomic resolution study of laccase inhibition by chloride and fluoride anions using single-crystal serial crystallography: Insights into the enzymatic reaction mechanism. *Acta Crystallographica Section D*, *75*(9), 804–816. https://doi.org/10.1107/S2059798319010684

Ramírez, E., Medina, E., Brenes, M., & Romero, C. (2014). Endogenous enzymes involved in the transformation of oleuropein in Spanish table olive varieties. *Journal of Agricultural and Food Chemistry*, *62*(39), 9569–9575. https://doi.org/10.1021/jf5027982

Rodríguez-López, J. N., Fenoll, L. G., García-Ruiz, P. A., Varón, R., Tudela, J., Thorneley, R. N. F., & García-Cánovas, F. (2000). Stopped-flow and steady-state study of the diphenolase activity of mushroom tyrosinase. *Biochemistry*, *39*(34), 10497–10506. https://doi.org/10.1021/bi000539+

Rodríguez-López, J. N., Gilabert, M. A., Tudela, J., Thorneley, R. N. F., & García-Cánovas, F. (2000). Reactivity of horseradish peroxidase compound II toward substrates: Kinetic evidence for a two-step mechanism. *Biochemistry*, *39*(43), 13201–13209. https://doi.org/10.1021/bi001150p

Rodríguez-López, J. N., Ros, J. R., Varón, R., & García-Cánovas, F. (1993). Oxygen Michaelis constants for tyrosinase. *Biochemical Journal*, *293*(3), 859–866. https://doi.org/10.1042/bj2930859

Sangha, A. K., Petridis, L., Cheng, X., & Smith, J. C. (2016). Relative binding affinities of monolignols to horseradish peroxidase. *The Journal of Physical Chemistry B*, *120*(31), 7635–7640. https://doi.org/10.1021/acs.jpcb.6b00789

Sanner, M. F. (1999). Python: A programming language for software integration and development. *Journal of Molecular Graphics and Modelling*, *17*(1), 57–61.

Schrödinger, L. (n.d.). *The PyMOL molecular graphics system* (2.3).

Segovia-Bravo, K. A., Jarén-Galán, M., García-García, P., & Garrido-Fernández, A. (2009). Browning reactions in olives: Mechanism and polyphenols involved. *Food Chemistry*, *114*(4), 1380–1385. https://doi.org/10.1016/j.foodchem.2008.11.017

Tikhonov, B. B., Sulman, E. M., Stadol'nikova, P. Y., Sulman, A. M., Golikova, E. P., Sidorov, A. I., & Matveeva, V. G. (2019). Immobilized enzymes from the class of oxidoreductases in technological processes: A review. *Catalysis in Industry*, *11*(3), 251–263. https://doi.org/10.1134/S2070050419030115

Tufarelli, V., Laudadio, V., & Casalino, E. (2016). An extra-virgin olive oil rich in polyphenolic compounds has antioxidant effects in meat-type broiler chickens. *Environmental Science and Pollution Research*, *23*(7), 6197–6204. https://doi.org/10.1007/s11356-015-5852-1

Vlasova, I. I. (2018). Peroxidase activity of human hemoproteins: Keeping the fire under control. *Molecules*, *23*(10), 2561. https://doi.org/10.3390/molecules23102561

Wallace, A. C., Laskowski, R. A., & Thornton, J. M. (1995). LIGPLOT: A program to generate schematic diagrams of protein-ligand interactions. *Protein Engineering, Design and Selection*, *8*(2), 127–134. https://doi.org/10.1093/protein/8.2.127

Xie, P., Fan, L., Huang, L., & Zhang, C. (2020). Oxidative polymerization of hydroxytyrosol catalyzed by laccase, tyrosinase or horseradish peroxidase: Influencing factors and molecular simulations. *Journal of Biomolecular Structure and Dynamics*, 1–12. Online ahead of print. https://doi.org/10.1080/07391102.2020.1801512

Xie, P., Fan, L., Huang, L., & Zhang, C. (2021). Oxidative polymerization process of hydroxytyrosol catalysed by polyphenol oxidases or peroxidase: Characterization, kinetics and thermodynamics. *Food Chemistry*, *337*, 127996. https://doi.org/10.1016/j.foodchem.2020.127996

Zolghadri, S., Bahrami, A., Hassan Khan, M. T., Munoz-Munoz, J., Garcia-Molina, F., Garcia-Canovas, F., & Saboury, A. A. (2019). A comprehensive review on tyrosinase inhibitors. *Journal of Enzyme Inhibition and Medicinal Chemistry*, *34*(1), 279–309. https://doi.org/10.1080/14756366.2018.1545767

SUPPORTING INFORMATION

Additional supporting information may be found online in the Supporting Information section.

How to cite this article: Manzano-Nicolas J, Taboada-Rodriguez A, Teruel-Puche JA, et al. Enzymatic oxidation of oleuropein and 3-hydroxytyrosol by laccase, peroxidase, and tyrosinase. *J Food Biochem*. 2021;45:e13803. https://doi.org/10.1111/jfbc.13803